JOURNAL OF THE AMERICAN COLLEGE OF CARDIOLOGY
© 2015 BY THE AMERICAN COLLEGE OF CARDIOLOGY FOUNDATION
PUBLISHED BY ELSEVIER INC.

VOL. 66, NO. 1, 2015
ISSN 0735-1097/$36.00
http://dx.doi.org/10.1016/j.jacc.2015.04.058

ORIGINAL INVESTIGATIONS

Electrophysiological, Electroanatomical, and Structural Remodeling of the Atria as Consequences of Sustained Obesity

Rajiv Mahajan, MD, PhD,* Dennis H. Lau, MBBS, PhD,* Anthony G. Brooks, PhD,* Nicholas J. Shipp, PhD,* Jim Manavis, PhD,† John P.M. Wood, D Phil,‡ John W. Finnie, BVSc, PhD,§ Chrishan S. Samuel, PhD,‖ Simon G. Royce, PhD,‖ Darragh J. Twomey, MBBS,* Shivshanker Thanigaimani, PhD,* Jonathan M. Kalman, MBBS, PhD,¶ Prashanthan Sanders, MBBS, PhD*

ABSTRACT

BACKGROUND Obesity and atrial fibrillation (AF) are public health issues with significant consequences.

OBJECTIVES This study sought to delineate the development of global electrophysiological and structural substrate for AF in sustained obesity.

METHODS Ten sheep fed ad libitum calorie-dense diet to induce obesity over 36 weeks were maintained in this state for another 36 weeks; 10 lean sheep with carefully controlled weight served as controls. All sheep underwent electrophysiological and electroanatomic mapping; hemodynamic and imaging assessment (echocardiography and dual-energy x-ray absorptiometry); and histology and molecular evaluation. Evaluation included atrial voltage, conduction velocity (CV), and refractoriness (7 sites, 2 cycle lengths), vulnerability for AF, fatty infiltration, atrial fibrosis, and atrial transforming growth factor (TGF)-β1 expression.

RESULTS Compared with age-matched controls, chronically obese sheep demonstrated greater total body fat ($p < 0.001$); LA volume ($p < 0.001$); LA pressure ($p < 0.001$), and PA pressures ($p < 0.001$); reduced atrial CV (LA $p < 0.001$) with increased conduction heterogeneity ($p < 0.001$); increased fractionated electrograms ($p < 0.001$); decreased posterior LA voltage ($p < 0.001$) and increased voltage heterogeneity ($p < 0.001$); no change in the effective refractory period (ERP) ($p > 0.8$) or ERP heterogeneity ($p > 0.3$). Obesity was associated with more episodes ($p = 0.02$), prolongation ($p = 0.01$), and greater cumulative duration ($p = 0.02$) of AF. Epicardial fat infiltrated the posterior LA in the obese group ($p < 0.001$), consistent with reduced endocardial voltage in this region. Atrial fibrosis ($p = 0.03$) and TGF-β1 protein ($p = 0.002$) were increased in the obese group.

CONCLUSIONS Sustained obesity results in global biatrial endocardial remodeling characterized by LA enlargement, conduction abnormalities, fractionated electrograms, increased profibrotic TGF-β1 expression, interstitial atrial fibrosis, and increased propensity for AF. Obesity was associated with reduced posterior LA endocardial voltage and infiltration of contiguous posterior LA muscle by epicardial fat, representing a unique substrate for AF.
(J Am Coll Cardiol 2015;66:1–11) © 2015 by the American College of Cardiology Foundation.

From the *Centre for Heart Rhythm Disorders (CHRD), South Australian Health and Medical Research Institute (SAHMRI), University of Adelaide and Royal Adelaide Hospital, Adelaide, Australia; †School of Medical Sciences, University of Adelaide, Adelaide, Australia; ‡Royal Adelaide Hospital and Department of Ophthalmology, University of Adelaide, Adelaide, Australia; §SA Pathology, Adelaide, Australia; ‖Department of Pharmacology, Monash University, Melbourne, Australia; and the ¶Department of Cardiology, Royal Melbourne Hospital and Department of Medicine, University of Melbourne, Melbourne, Australia. Dr. Mahajan is supported by the Leo J. Mahar Lectureship from the University of Adelaide. Dr. Lau is supported by a postdoctoral fellowship

ABBREVIATIONS AND ACRONYMS

AF = atrial fibrillation
BP = blood pressure
CL = cycle length
CoV = coefficient of variation
CS = coronary sinus
ERP = effective refractory period
HE = hematoxylin and eosin
IQR = interquartile range
LA = left atrium/atrial
LAA = left atrial appendage
LV = left ventricular
OSA = obstructive sleep apnea
PA = pulmonary artery
RA = right atrium/atrial
TGF = transforming growth factor

Atrial fibrillation (AF) is an important health problem, with 2010 global estimates suggesting that it affects 33.5 million individuals (1). This prevalence is projected to increase 2.5-fold by 2050 (2). Emerging evidence suggests that aging alone does not account for the exponential rise in AF prevalence (2). It is in this setting that new risk factors, such as obesity, have been proposed as important contributors to this epidemic (3). Obesity is a rampant epidemic, with more than one-third of the population being overweight or obese. Analysis of population-based studies suggests that obesity is associated with long-term increased risk of AF, independent of other risk factors (4–6). In a meta-analysis by Wanahita et al. (7), there was a graded dose-response relationship between obesity and AF in the general population.

SEE PAGE 12

The mechanisms by which obesity predisposes to AF are confounded by the coexistence of obstructive sleep apnea (OSA), hypertension, diabetes, and coronary artery disease, all well-established precursors for the development of AF. Using limited, open-chest, direct contact mapping, we have previously shown conduction slowing and atrial fibrosis with short-term weight gain in an ovine model (8). In the present study, we investigate the global endocardial electrophysiological, electroanatomic, and structural substrate with sustained obesity, a state more comparable with humans.

METHODS

The animal research ethics committees of the University of Adelaide and the South Australian Health and Medical Research Institute, Adelaide, Australia, which adhere to the National Health and Medical Research Council of Australia Guidelines for the Care and Use of Animals for Research Purposes, approved the study.

OBESE OVINE MODEL. A total of 10 sheep had obesity induced through a previously described protocol using an ad libitum regimen of hay and high-energy pellets (9). At baseline, healthy sheep were commenced on a high-calorie diet of energy-dense soybean oil (2.2%) and molasses-fortified grain and maintenance hay with weekly weight measurement. Excess voluntary intake was predominantly of grass alfalfa silage and hay. For the obese sheep, pellets were gradually introduced at 8% excess basal energy requirements, and rationed to ≥70% of total dry-matter intake. Blood samples were periodically collected to ensure electrolyte and acid-base homeostasis. The sheep gradually gained weight, reaching maximal obesity at 36 weeks and were subsequently maintained in this state for a further 36 weeks.

CONTROL GROUP. Ten age-matched sheep were maintained as controls at their baseline weight. To do this, high-quality hay was provided ad libitum, while energy-dense pellets were rationed at 0.75% of body weight. The nutritional content of food and housing conditions were identical for both groups, with only the amount of food intake varying.

STUDY PREPARATION. Animals were pre-acclimatized for at least 1 week before any surgery. Shorn weight was recorded immediately before surgery.

BODY COMPOSITION. Dual-energy x-ray absorptiometry scans were performed to determine total body fat in the animals.

TRANSTHORACIC ECHOCARDIOGRAPHY. An echocardiogram (Acuson Aspen, Siemens Healthcare, Malvern, Pennsylvania) was performed under general anesthesia before the electrophysiology study. The left atrial (LA) dimensions were measured in the

from the National Health and Medical Research Council of Australia (NHMRC). Drs. Brooks and Sanders are supported by the National Heart Foundation of Australia. Dr. Samuel is supported by an NHMRC Senior Research Fellowship. Dr. Twomey is supported by the Leo J. Mahar Electrophysiology Scholarship from the University of Adelaide. Dr. Thanigaimani is supported by the Peter Hetzel Electrophysiology Scholarship from the University of Adelaide. Dr. Kalman is supported by a Practitioner Fellowship from the NHMRC; and has received research funding from St. Jude Medical, Biosense Webster, Medtronic, and Boston Scientific. Dr. Sanders is supported by a Practitioner Fellowship from the NHMRC; has served on the advisory boards of Biosense Webster, Medtronic, St. Jude Medical, Sanofi, and Merck, Sharpe and Dohme; has received lecture and/or consulting fees from Biosense Webster, Medtronic, St. Jude Medical, Boston Scientific, Merck, Sharpe and Dohme, Biotronik, and Sanofi; and has received research funding from Medtronic, St. Jude Medical, Boston Scientific, Biotronik, and Sorin. All other authors have reported that they have no relationships relevant to the contents of this paper to disclose. Previously presented at the Annual Scientific Sessions of the Heart Rhythm Society, May 2012, Boston, Massachusetts, and published in abstract form (Heart Rhythm 2012;9:S185). Drs. Lau and Sanders contributed equally to this paper.
Listen to this manuscript's audio summary by *JACC* Editor-in-Chief Dr. Valentin Fuster.

Manuscript received February 3, 2015; revised manuscript received March 29, 2015, accepted April 24, 2015.

apical 4-chamber view. The left ventricular (LV) dimensions were measured in M-mode in parasternal long-axis view at the level of mitral leaflet tips. The LV dimensions were utilized for determination of global LV function by the Teicholz formula.

HEMODYNAMIC ASSESSMENT. Invasive blood pressure (BP) monitoring was performed during the electrophysiology study. LA, right atrial (RA), and pulmonary artery (PA) pressures were recorded.

ELECTROPHYSIOLOGICAL STUDY. Details of the electrophysiological study are presented in the Online Appendix and are based on previously published methodology (10). Briefly, venous access was obtained through the right femoral and left internal jugular veins. A 10-pole catheter was advanced to the coronary sinus (CS). A conventional trans-septal puncture was performed using a BRK1 needle and SL0 sheath to access the left atrium. A 3.5-mm tip catheter (Navistar, Biosense Webster, Diamond Bar, California) was used to create electroanatomic maps of the RA and LA in sinus rhythm with the CARTO XP mapping system (Biosense Webster). The following were determined:

Effective refractory period. The effective refractory period (ERP) was measured from the following 7 sites: 1) RA appendage; 2) RA lateral wall, upper; 3) RA free wall, lower; 4) proximal CS; 5) distal CS; 6) LA appendage (LAA); and 7) LA posterior wall. ERP heterogeneity was determined by the coefficient of variation (CoV) of ERP variation at each cycle length (CL) (CoV = SD/mean × 100%).

AF vulnerability and duration. AF vulnerability was assessed during ERP testing. AF was defined as rapid, irregular atrial activity lasting ≥2 s. AF lasting more than 10 min was considered sustained; when this occurred, no further data were acquired.

Electroanatomic mapping. Electroanatomic maps of the LA/RA were created in sinus rhythm using the CARTO (Biosense Webster) mapping system. Details of the electroanatomic mapping and analysis are presented in the Online Appendix and are based on previously published methodology (10). Each point was binned according to location (region), fractionation (presence or absence), scar (presence or absence), and bipolar voltage amplitude to allow analysis in a mixed-effects model. Regional atrial bipolar voltage and conduction velocity were analyzed off-line. The LA/RA maps were segmented for analysis, and the following parameters were assessed as previously described (11):

1. Atrial conduction velocity: Conduction velocity for each segment was determined by averaging the conduction velocity between 3 to 5 pairs of points. An index of heterogeneity was determined by calculating the CoV of the different regions in each chamber.
2. Electrograms with a duration ≥50 ms and 3 or more deflections crossing baseline were considered complex fractionated electrograms; and double potentials were potentials separated by an isoelectric interval and with a total electrogram duration ≥50 ms. For analysis, a fraction of the total number of fractionated/double points was utilized.
3. Atrial voltage: Low-voltage areas were defined as 3 contiguous points with a bipolar voltage <0.5 mV. Electrically silent areas (scar) were defined as 3 contiguous points with an absence of recordable activity or bipolar voltage amplitude <0.05 mV. An index of heterogeneity was determined by calculating the CoV of the different regions in each chamber.

HISTOLOGICAL ASSESSMENT. Isolated atrial tissues from the LA posterior wall and LAA were perfusion-fixed with 4% paraformaldehyde and immersed in 10% buffered formalin. Sections were processed and embedded in paraffin. For each site, 5-μm serial sections were then taken at 1-cm intervals from each block and stained with hematoxylin and eosin (HE) and Masson's trichrome, respectively. Additional samples were frozen at −70°C.

Fatty infiltration of atrial muscle by epicardial fat. Fat infiltration of the atrial muscle from the epicardial fat was evaluated in low-power (1.25×) magnification with hematoxylin and eosin staining and confirmed with Oil Red O staining of frozen sections. Fatty infiltration of the atrium by the overlying

TABLE 1 Structural and Hemodynamic Characteristics of the Control and Obese Groups

	Controls	Obese	p Value
Weight, kg	60 ± 7	110 ± 9	<0.001
Total body fat, kg	9 ± 6	35 ± 6	<0.001
Total body fat/total soft tissue (DEXA)	15.2 ± 7.8	36.9 ± 4.3	<0.001
LA major axis, mm	36.2 ± 1.3	38.3 ± 1.9	0.01
LA minor axis, mm	27.7 ± 1.1	30.1 ± 1.4	<0.001
LV posterior wall, mm	7.1 ± 0.6	8.8 ± 1.2	0.001
LVEF, %	67 ± 5	70 ± 6	0.8
LA pressure, mm Hg	3.7 ± 1.4	8.1 ± 1.6	<0.001
RA pressure, mm Hg	1.8 ± 1.1	4.6 ± 1.2	<0.001
PA pressure, mm Hg	9.8 ± 2.6	15.0 ± 0.9	<0.001
Systemic mean BP, mm Hg	71 ± 12	86 ± 13	0.02

Values are mean ± SD.

BP = blood pressure; DEXA = dual-energy x-ray absorptiometry; LA = left atrial; LV = left ventricle/ventricular; LVEF = left ventricular ejection fraction; PA = pulmonary artery; RA = right atrium.

TABLE 2 Electrophysiological and Structural Characteristics of the Control and Obese Groups

	Controls	Obese	p Value
LA CARTO volume, ml	74 ± 13	86 ± 15	<0.001
RA CARTO volume, ml	75 ± 15	89 ± 16	<0.001
FP/DP LA, %	10.8 ± 4.4	53.3 ± 13.6	<0.001
FP/DP RA, %	8.2 ± 2.8	36.0 ± 12.3	<0.001
CV, LA, m/s	1.58 ± 0.22	1.18 ± 0.28	<0.001
CV, RA, m/s	1.43 ± 0.16	1.02 ± 0.24	<0.001
Conduction heterogeneity, %	9.1 ± 4.9	22.0 ± 6.1	<0.001
Voltage LA, mV	4.4 ± 1.4	4.5 ± 1.7	0.3
Voltage RA, mV	3.6 ± 0.9	4.1 ± 1.6	0.3
Voltage heterogeneity, %	24.6 ± 7.5	32.1 ± 8.8	<0.001
ERP mean, ms, CL 300 ms	182 ± 18	180 ± 19	0.8
ERP heterogeneity at CL 300 ms, %	10.0 ± 4.2	10.5 ± 3.3	0.7
ERP mean, ms, CL 450 ms	190 ± 20	191 ± 26	1.0
ERP heterogeneity at CL 450 ms, %	10.3 ± 3.3	13.6 ± 5.4	0.3
AF episodes, total	1 (0–2)	4.5 (2–7)	0.02
Cumulative AF duration, s	4.1 (3–15)	46 (10–112)	0.02
Atrial fibrosis, %	5.31 ± 0.95	8.14 ± 2.39	0.03
Atrial TGF-β1 protein	0.35 ± 0.23	2.07 ± 1.24	0.002
Fatty infiltration grade* posterior LA	1.0 ± 0.0	2.5 ± 0.7	<0.001
Fatty infiltration grade* LAA	1.0 ± 0.0	1.2 ± 0.4	0.18

Values are mean ± SD or median (interquartile range). *See text under histological assessment.

AF = atrial fibrillation; CARTO = CARTO XP mapping system (Biosense Webster); CL = cycle length; CV = conduction velocity; DP = double potentials; ERP = effective refractory period; FP = fractionated potentials; IQR = interquartile range; LAA = left atrial appendage; TGF = transforming growth factor; other abbreviations as in Table 1.

FIGURE 1 Distribution of ERP in Obese and Control Groups

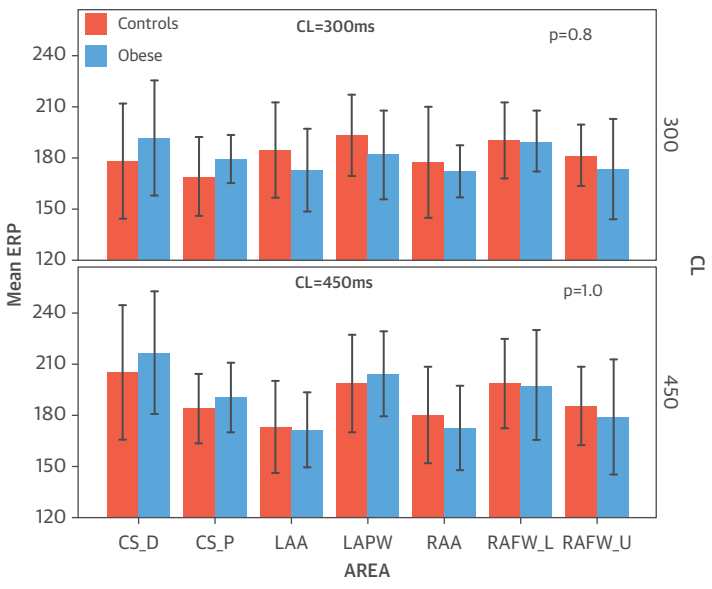

The **top and bottom** depict ERP at 300 and 450 ms CL, respectively. CL = cycle length; CS = coronary sinus; CS_D = distal coronary sinus; CS_P = proximal coronary sinus; ERP = effective refractory period; LAA = left atrial appendage; LAPW = left atrial posterior wall; RAA = right atrial appendage; RAFW_U = upper right atrial free wall; RAFW_L = lower right atrial free wall.

epicardial adipose tissue was graded 1 to 3 on the basis of severity as follows:

1. None or focal infiltration of the adjacent outer third of the atrial muscle layer by the overlying epicardial adipose tissue.
2. Coalescent infiltration of the outer third and/or focal infiltration up to the middle third of the atrial muscle layer.
3. Coalescent infiltration extending from the epicardial adipose tissue to the middle or inner third of the atrial muscle layer.

Fibrosis assessment. Morphometric analysis of Masson's trichrome-stained sections to obtain a quantitative estimate of collagen within the tissue (described in the Online Appendix).

Atrial TGF-β1 assessment. Western blotting was used to assess changes in transforming growth factor (TGF)-β1 tissue expression in LA myocardium (described in the Online Appendix).

STATISTICAL ANALYSIS. Normally distributed continuous data were expressed as mean ± SD and tested with unpaired Student *t* tests between groups. Skewed distributions were expressed as median and interquartile range (IQR) and means tested using Mann-Whitney *U* tests. Mixed-effect models were fitted to the data in order to compare voltage, conduction velocity, fractionation, and atrial refractory period across regions, chambers, and groups (obese and control). Fixed effects included combinations of group (obese, control), region, and chamber (LA/RA) with a maximum of 2 fixed effects entered into the statistical model at a time. Main effects and their interaction were tested. Random effects of sheep identity were fitted to all models to account for dependence on observations from the same animal. To investigate LA regional patterns in both approaches, region (posterior LA, anterior LA, septal LA, inferior LA, lateral LA, and LA roof) and group (obese and control) were modeled as fixed effects with an interaction term (region · group). If a significant interaction was present, mixed-effects post-hoc test p values were reported (with Sidak adjustment of alpha level). In the case of skewed distribution (i.e., for fibrosis assessment with Masson's trichrome staining), data were log-transformed before further analysis. Two-sided p values <0.05 were considered statistically significant. All analyses were performed using SPSS/PASW version18 (SPSS, Chicago, Illinois).

RESULTS

GROUP CHARACTERISTICS. The obese sheep achieved peak weight over a period of 36 weeks and remained

in this state of sustained obesity for another 36 weeks. The control sheep were maintained lean during this period. The obese sheep were twice the weight of the control animals and had significantly greater total body fat. Table 1 presents the characteristics of the 2 groups.

STRUCTURAL AND HEMODYNAMIC REMODELING. Table 1 details the hemodynamic characteristics of the 2 groups. The LA was enlarged ($p = 0.01$) with increases in LA pressure ($p < 0.001$) without a change in LV ejection fraction ($p = 0.8$) in the obese sheep, as compared with the controls. In addition, there was a significant increase in RA and PA pressures ($p < 0.001$) with obesity. Systemic BP was also elevated in the obese animals, as compared with the controls ($p = 0.02$).

ELECTROPHYSIOLOGICAL AND ELECTROANATOMIC REMODELING. Electroanatomic maps of the atria were created in sinus rhythm. Table 2 summarizes the electrophysiological findings. LA and RA volumes

FIGURE 2 Atrial Conduction Abnormalities With Chronic Obesity

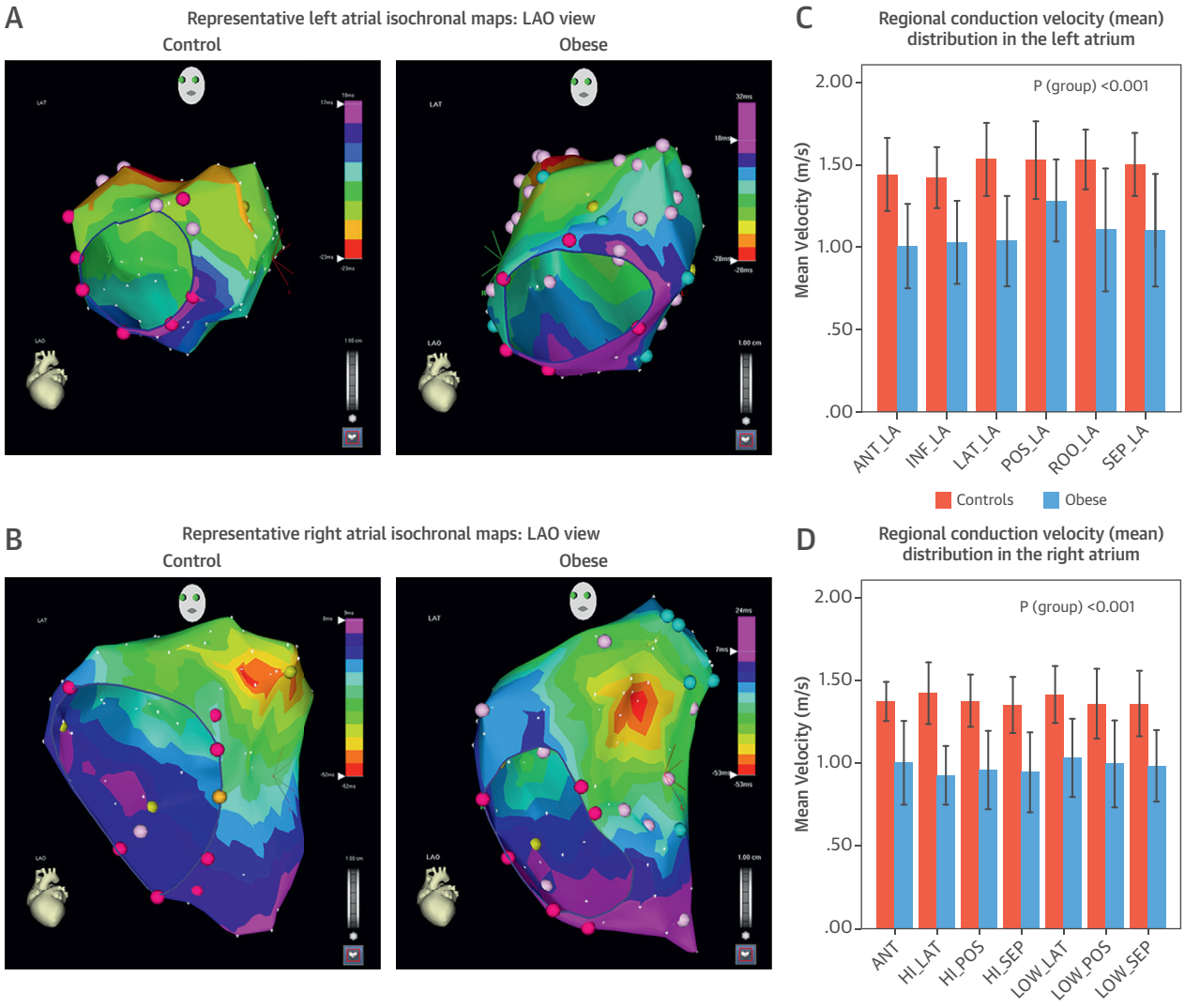

(A and B) Representative LA and RA isochronal maps (5 ms), respectively, demonstrating conduction in obese and control groups in sinus rhythm. The isochrones in the obese sheep are more crowded and greater time was required to activate the atria. **(C and D)** Regional distributions of conduction velocity (mean) of the LA and RA, respectively. Conduction velocity was uniformly reduced across all regions. ANT = anterior; ANT_LA = anterior left atrium; HI_LAT = high lateral; HI_POS = high posterior; HI_SEP = high septal; INF_LA = inferior left atrium; LA = left atrium; LAO = left anterior oblique; LAT_LA = lateral left atrium; LOW_LAT = low lateral; LOW_POS = low posterior; LOW_SEP = low septal; POS_LA = posterior left atrium; RA = right atrium; ROO_LA = left atrial roof; SEP_LA = septal left atrium.

were increased in the obese sheep, as compared with the controls ($p < 0.001$).

ATRIAL REFRACTORINESS. Atrial ERPs, at CLs of 450 and 300 ms, from the 7 sites did not differ significantly between the 2 groups (CL 300 ms, $p = 0.8$; CL 450 ms, $p = 1.0$) (Table 2, Figure 1). ERP heterogeneity at CLs of 450 and 300 ms also did not significantly differ between the obese and control groups (CL 300 ms, $p = 0.7$; CL 450 ms, $p = 0.3$).

CONDUCTION VELOCITY. The mean conduction velocity was significantly reduced in the obese group in both atrial chambers (LA 1.18 ± 0.04 m/s and RA 1.02 ± 0.04 m/s), as compared with the controls (LA 1.58 ± 0.04 m/s and RA 1.43 ± 0.04 m/s; $p < 0.001$)

FIGURE 3 Atrial Voltage Abnormalities With Chronic Obesity

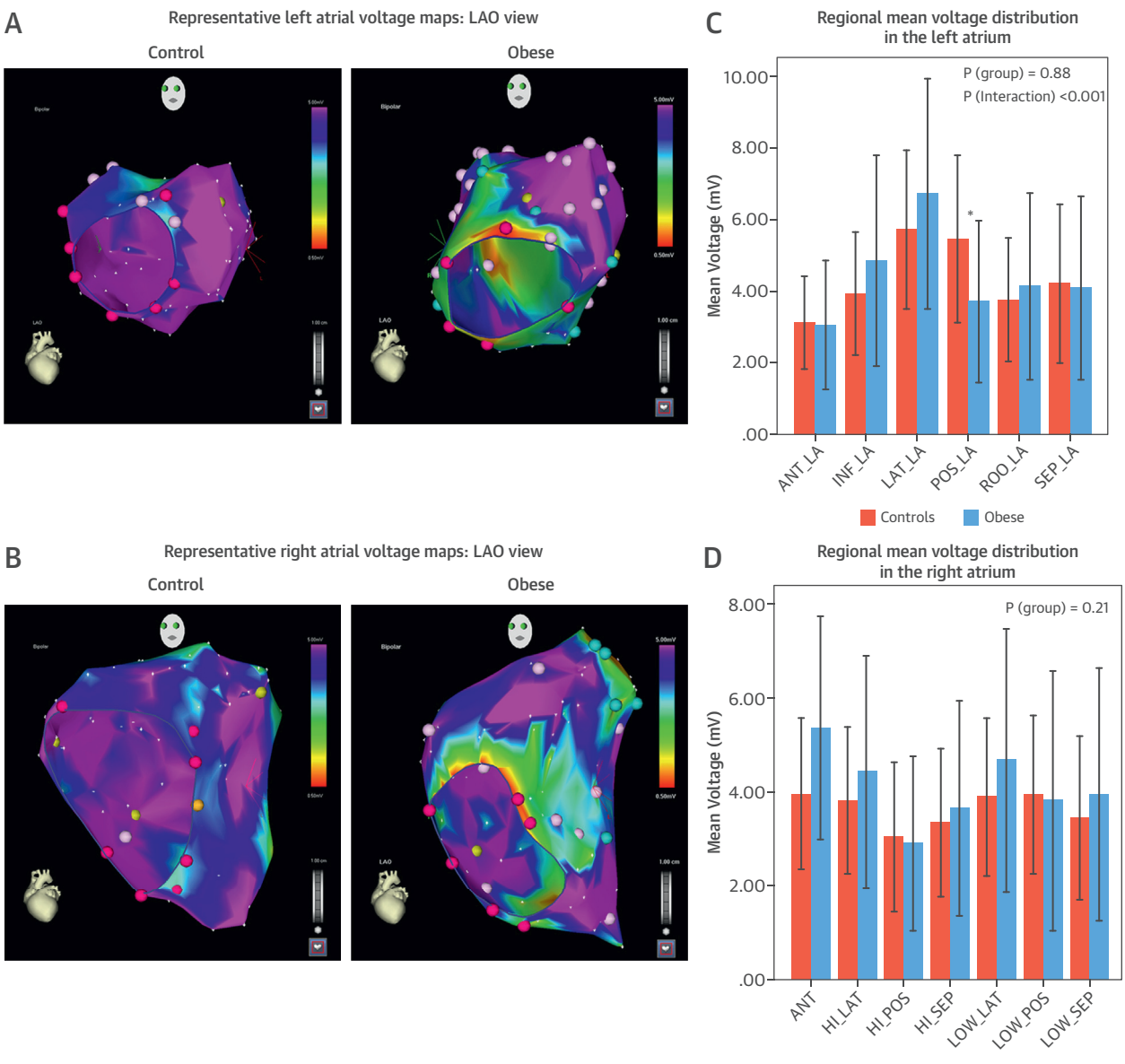

(A and B) Representative LA and RA voltage (bipolar) maps, respectively, of obese and control groups in sinus rhythm. The voltage range was selected manually with the lower limit set at 0.5 mV and the upper limit at 5.0 mV. Note the heterogeneity in the voltage and increased fractionated/double potentials **(colored dots)** in the obese animal. There was absence of electrical scar. **(C and D)** Regional distribution of voltage (mean) of the LA and RA, respectively, in the 2 groups. The voltage in the posterior LA was reduced (*$p < 0.001$) in the obese group. Abbreviations as in Figure 2.

(Figure 2). The reduction in conduction velocity was consistent across different LA segments (interactive p value [area × group] = 0.6). In addition, conduction was more heterogeneous in the obese as compared with the controls (CoV: 22.0 ± 6.1% vs. 9.1 ± 4.9%; $p < 0.001$) (Figure 1). After adjusting for changes in LA pressure, the differences in conduction velocity ($p < 0.001$) and heterogeneity ($p < 0.001$) persisted in obese animals compared with controls.

COMPLEX FRACTIONATION. The LA demonstrated greater fractionation/double potentials, as compared with the RA in both the obese and control groups ($p < 0.001$). During sinus rhythm, 53.2 ± 13.6% and 36.0 ± 12.3% of LA and RA signals, respectively, were fractionated/double potentials in the obese group. By contrast, only 10.8 ± 4.4% and 8.2 ± 2.8% of all LA and RA signals, respectively, were fractionated/double potentials in the control group ($p < 0.001$).

VOLTAGE. The mean global voltage did not differ between obese (LA 4.5 ± 1.7 mV; RA 4.1 ± 1.6 mV) and control groups (LA 4.4 ± 1.4 mV, p = 0.88; RA 3.6 ± 0.9, p = 0.21) (Figure 3). There were no areas of scar in either chamber in control or obese animals. However, the LA regional voltage patterns were different (interaction $p < 0.001$) in the obese and control groups, primarily due to a significant reduction in the posterior LA voltage (3.7 ± 2.3 mV vs. 5.5 ± 2.3 mV; $p < 0.001$) in the obese. Regional voltage heterogeneity was elevated in the obese group, as compared with the controls (CoV: 32.1 ± 8.8% vs. 24.6 ± 7.5%; $p < 0.001$).

VULNERABILITY FOR AF. The median number of AF episodes was greater in the obese group, as compared with controls (4.5 [IQR: 2 to 7] vs. 1 [IQR: 0 to 2]; p = 0.02). The total AF episode duration per animal was increased in the obese group as compared with the controls (46 [IQR: 10 to 112] s vs. 4.1 [IQR: 3 to 15] s; p = 0.05). Similarly, the average AF episode length was longer in the obese as compared with control animals (7.9 [IQR: 5 to 17.7] s vs. 2.7 [IQR: 2 to 5] s; p = 0.01).

ATRIAL MUSCULATURE INFILTRATION BY EPICARDIAL ADIPOSE TISSUE. Distribution of epicardial adipose tissue. In relation to the atria, epicardial adipose tissue was distributed adjacent to the LA posterior wall and atrioventricular groove (Figure 4), with minimal epicardial adipose tissue adherent to the appendage. By contrast, paracardial adipose tissue was more diffuse in distribution, with prominent deposits between the appendage and great arteries.

Fatty infiltration by epicardial fat. In control sheep, limited numbers of adipocytes were present subepicardially, interposed between cardiac myocytes, whereas in obese animals, adipocyte hyperplasia resulted in abundant deposition of adipose tissue in the epicardium and infiltration into the atrial musculature. Moderate (Grade II) to severe (Grade III) LA posterior wall infiltration by overlying epicardial fat was seen significantly more in the obese sheep (mean grade: obese 2.5 ± 0.7, controls 1.0 ± 0.0; $p < 0.001$). There was minimal fatty infiltration in the LAA in both groups (p = 0.18; mean grade: 1.2 ± 0.4 and 1 ± 0 for obese and control groups, respectively). Grade III fatty infiltration was not seen in the LAA in either group, where epicardial fat was minimal. Figure 4 depicts representative HE-stained sections (1.25×), demonstrating fatty infiltration of the atrial musculature by epicardial adipose tissue in the obese and control groups.

FIBROSIS. There was increased interstitial fibrosis in the obese animals, as compared with the control animals (p = 0.03; on log-transformed data).

FIGURE 4 Epicardial Fat: Novel Substrate for AF in Chronic Obesity

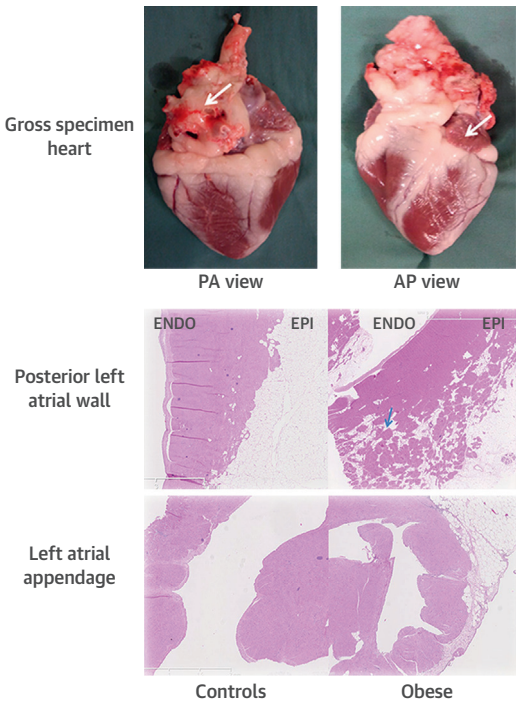

(Top) Gross specimen of sheep heart after removal of parietal pericardium with pericardial fat. PA view: **arrow** points to epicardial fat adjacent to the LAPW. AP view: **arrow** points to the LAA, which has very little epicardial fat. **(Middle and Bottom)** Representative H&E stained sections (1.25×) of the LAPW and LAA, respectively, from control and obese groups. **Arrow** shows infiltration of atrial musculature with fat cells. AF = atrial fibrillation; AP = anterior-posterior; ENDO = endocardial; EPI = epicardial; H&E = hematoxylin and eosin; PA = posterior-anterior; other abbreviations as in Figure 1.

FIGURE 5 Fibrosis and Profibrotic TGFβ1 Expression With Chronic Obesity

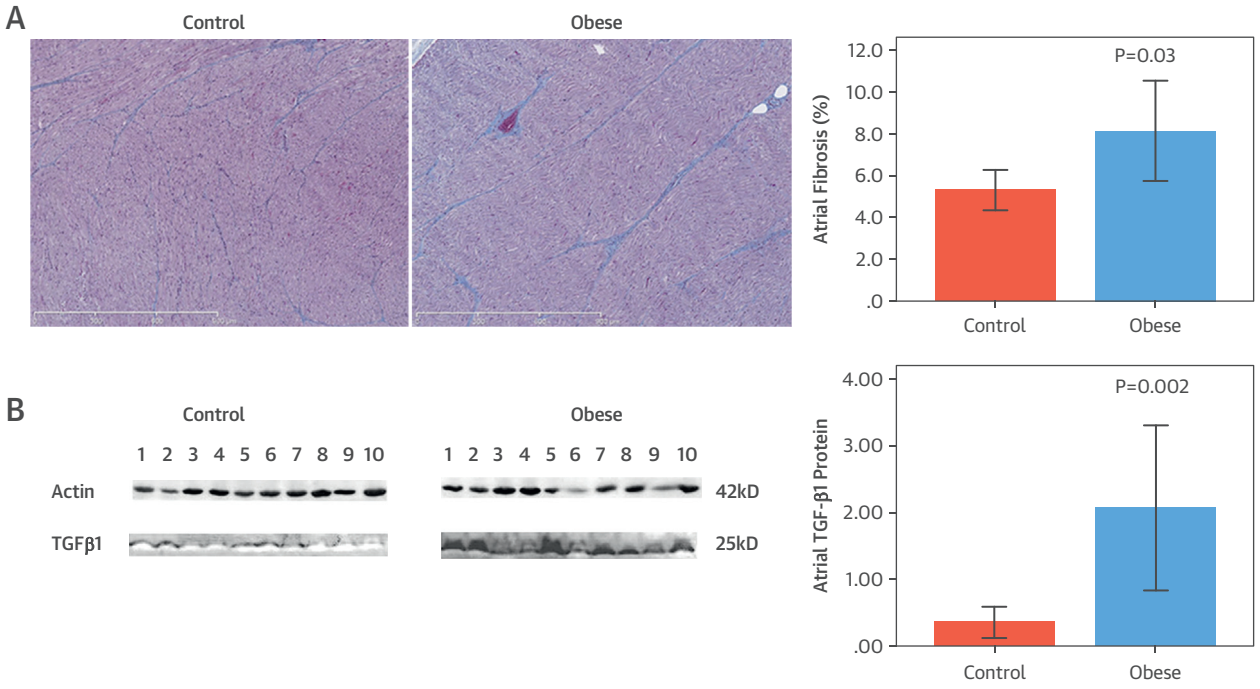

(A) Representative Masson's trichrome-stained sections (5×) of the left atrial (LA) posterior wall. The **bar graph** demonstrates the degree of atrial fibrosis in the control and obese groups. The fibrous tissue is stained **blue** and assessed morphometrically. **(B)** Western blots for TGF-β1 expression in LA tissue. The **bar graph** demonstrates atrial TGF-β1 protein expression in control and obese groups. TGF = transforming growth factor.

Morphometric analysis of the Masson's trichrome-stained LA sections demonstrated 8.14 ± 2.39%, and 5.31 ± 0.95% staining in the obese and control groups, respectively. Figure 5A shows representative Masson's trichrome-stained sections from the 2 groups.

ATRIAL TGF-β1 PROTEIN. Atrial TGF-β1 protein expression increased 5-fold in the obese group, as compared with the control group ($p = 0.001$ on log-transformed data) (Figure 5B, Table 2).

DISCUSSION

MAJOR FINDINGS. This study presents new information on the global endocardial electrophysiological, electroanatomic remodeling, and fatty infiltration of the atria as a result of sustained obesity. Animals gained weight over 36 weeks to achieve stable obesity and maintained this for another 36 weeks to replicate a state more comparable with chronic obesity in humans. The obese group accumulated 5-fold greater total body fat (34.5 kg), as compared with controls (8.7 kg). The obese sheep model is unique, because it does not experience OSA, because of the typical habitus and sleeping posture, thereby excluding the confounding effects of OSA. It demonstrates the following.

Structural and hemodynamic changes

- Biatrial enlargement with diastolic dysfunction, reflected by elevated LA pressure in the presence of normal ventricular function
- Elevated right heart pressures and systemic BP
- Increased expression of profibrotic TGF-β1 and increased interstitial fibrosis
- Fat infiltration of the atrial myocardium

Electrophysiological remodeling

- Slowed and heterogeneous conduction
- Increased complex fractionated electrograms
- Increased voltage heterogeneity without significant change in mean voltage or appearance of scar/low voltage
- No change in ERP and ERP heterogeneity

As a result of these hemodynamic, structural, and electrophysiological changes, obese animals were more vulnerable to AF. Importantly, this study provides causative evidence that links obesity directly with the development of the AF substrate.

CENTRAL ILLUSTRATION **Obesity and the Substrate for AF**

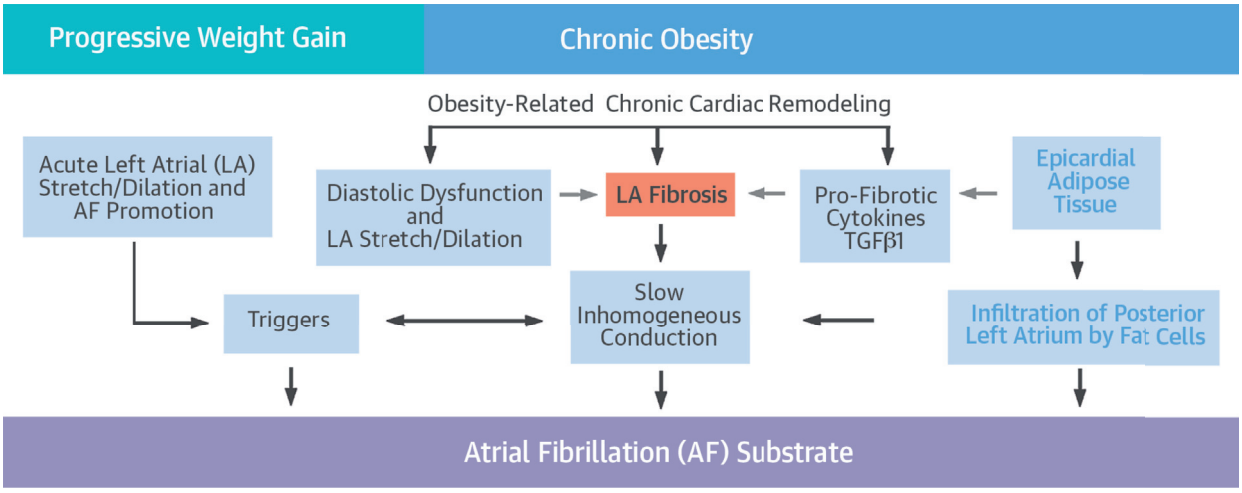

Mahajan, R. et al. J Am Coll Cardiol. 2015; 66(1):1–11.

Progressive weight gain has been demonstrated to result in atrial stretch and leads to the development of high-frequency triggers and the substrate for AF. With chronic obesity, there is greater epicardial adipose tissue, activation of the cytokines, and the development of fibrosis. In addition, there is infiltration of the contiguous atrial myocardium by fat cells. All of these result in the milieu of slowed and inhomogeneous conduction that forms the substrate for AF. AF = atrial fibrillation; LA = left atrial; TGF = transforming growth factor.

ATRIAL SUBSTRATE PRE-DISPOSING TO AF. Over the last decade, several studies have presented evaluations of the atrial substrate in conditions known to result in AF. Li et al. (12) were the first to distinguish these abnormalities forming the "second factor" from the electrical remodeling associated with AF. They highlighted the importance of conduction abnormalities and structural changes, particularly diffuse atrial fibrosis in an experimental heart failure model (12). These findings were subsequently confirmed to be the unifying feature of structural remodeling in other conditions, in both pre-clinical studies (13-15) and clinical studies (10,11,16,17).

AF SUBSTRATE IN OBESITY. Although an epidemiological link has been established between obesity and AF, the underlying electrophysiological changes and mechanism still remain to be defined (4-6). OSA is closely associated with obesity in humans and predisposes to AF by causing hypertension, diastolic dysfunction, LA stretch, and autonomic imbalance during sleep. Iwasaki et al. (18) demonstrated that obesity facilitates AF inducibility in the presence of acute OSA. However, despite the structural remodeling, AF inducibility was not enhanced in obese rats in the absence of obstruction. The ovine model allows evaluation of obesity in the absence of OSA and, in this study, demonstrated diffuse conduction abnormalities and interstitial fibrosis with chronic obesity alone. The **Central Illustration** summarizes the structural changes that result in electrical remodeling and promote AF in obesity.

Global endocardial biatrial conduction slowing and increased fractionation were demonstrated in chronically obese animals. However, the degree of slowing varied in different regions, resulting in increased conduction heterogeneity. This is consistent with the finding with limited epicardial mapping with short-term weight gain in an ovine model (8). Munger et al. (19) have also reported slowed longitudinal conduction velocities from the LA to the pulmonary veins in obese patients with AF. However, this human study did not observe any change in conduction velocity along the coronary sinus. The more pronounced findings in our animal model may result from extreme obesity and more detailed mapping. The obese animals did not demonstrate electrical scars or alterations in global voltage; however, there was reduction in posterior LA voltage with increased voltage heterogeneity. Contiguous epicardial fat was observed to infiltrate the region demonstrating the voltage reduction. Thus, we hypothesize that fatty infiltration of the posterior LA by epicardial fat could potentially represent a unique substrate that could

predispose to AF in obesity. As with other studies evaluating clinical substrate for AF, endocardial atrial refractoriness was not altered with sustained obesity. This finding differs from that of Munger et al., who reported shortened atrial refractoriness in obese patients undergoing ablation for AF. However, they acknowledged that AF induced during ERP testing could potentially affect atrial refractoriness. In addition, a marked increase in complex fractionated signals was observed with sustained obesity in our study. This could be a result of conduction slowing secondary to interstitial fibrosis or fat infiltration.

Sustained obesity was associated with diffuse atrial interstitial fibrosis. This is consistent with changes observed with heart failure (12,20) and chronic hypertension (14). Spach et al. (21) have demonstrated elegantly that fibrosis can produce conduction abnormalities promoting re-entry and AF. The fibrosis observed in their study was only interstitial in nature, without the areas of replacement fibrosis usually seen with infarction. Moreover, there was only a 50% increase in interstitial fibrous tissue, in comparison to the 16-fold increase observed with heart failure (12), suggesting a more subtle insult with obesity.

TGF-β1 has been shown to be a crucial cytokine in the signal transduction pathways responsible for fibrosis. It occupies a central position, downstream of angiotensin and upstream of endothelin pathways, and acts in a paracrine-autocrine fashion. Verheule et al. (22) have shown that overexpression of constitutional TGF-β1 in transgenic mice led to selective atrial fibrosis, conduction heterogeneity, and AF. In our study, TGF-β1 expression was increased 5-fold with sustained obesity and could explain the increase in interstitial fibrosis. We have previously reported increased endothelin receptor expression with short-term weight gain (8). There are similar reports of TGF-β superfamily (23) and endothelin (24) signaling pathway overexpression in humans.

EPICARDIAL FAT AND AF. There is emerging evidence that localized epicardial fat depots may have a significant and independent role in development of AF (25–28). The development of the obese state has been shown to be associated with hypoxia of the expanding adipose tissue, resulting in adipose tissue fibrosis and production of a myriad of adipocytokines, including those in the TGF-β superfamily (29). The absence of fascial barriers between epicardial fat and the contiguous atrial musculature, and the common vascular supply may facilitate paracrine action. Venteclef et al. (30) elegantly demonstrated paracrine action in an organ-culture model. They incubated rat atrial tissue in a secretome derived from human epicardial fat and demonstrated atrial fibrosis mediated by members of the TGF-β superfamily. We demonstrated several-fold increased expression of TGF-β1 in atrial tissue; however, the source was not evaluated. In addition, a new finding was observed with epicardial fat infiltrating the underlying myocardium. Epicardial fat is predominantly deposited on the posterior LA. The reduction in posterior LA voltage noted on endocardial mapping was consistent with this finding. We hypothesize that fat infiltration separates myocytes and could result in conduction abnormalities in a fashion similar to microfibrosis (21). Considering the infiltration was observed only adjacent to epicardial fat deposits, the distribution of epicardial fat could contribute to conduction heterogeneity.

STUDY LIMITATIONS. Although the observed electrical and structural abnormalities predispose to AF, the development of clinical AF is a complex process, with other factors, such as triggers and perpetuators, not addressed in the current study. This study has shown that epicardial fat cells infiltrate the posterior LA. However, a causal relationship between fatty infiltration and AF vulnerability could only be studied to a limited extent in this model. Furthermore, the profibrotic signal transducing pathways responsible for AF in obesity were not fully elucidated.

CONCLUSIONS

Sustained chronic obesity results in chronic stretch, diffuse interstitial fibrosis, conduction abnormalities, and increased vulnerability to AF. A TGF-β signaling pathway may play an important role in mediating interstitial fibrosis in sustained obesity. Infiltration of the underlying atrial musculature by epicardial fat may be a unique feature of the AF substrate in obesity. This study provides direct evidence for the role of obesity in development of a unique substrate predisposing to AF.

ACKNOWLEDGMENT The authors acknowledge the contribution of Mr. Krupesh Patel for the morphometric analysis of inflammation and fibrosis.

REPRINT REQUESTS AND CORRESPONDENCE: Dr. Prashanthan Sanders, Centre for Heart Rhythm Disorders (CHRD), Department of Cardiology, Royal Adelaide Hospital, Adelaide, SA 5000, Australia. E-mail: prash.sanders@adelaide.edu.au.

PERSPECTIVES

COMPETENCY IN MEDICAL KNOWLEDGE: Sustained obesity, in the absence of sleep apnea, is associated with diastolic ventricular dysfunction, elevation of atrial profibrotic TGF-β1, infiltration of atrial musculature by contiguous epicardial fat, and atrial fibrosis. These factors contribute to electrophysiological remodeling and AF.

TRANSLATIONAL OUTLOOK: Further studies are needed to determine whether therapies that inhibit fat cell infiltration from the epicardial depot into the left atrial wall of obese individuals could reduce their risk of developing AF.

REFERENCES

1. Chugh SS, Havmoeller R, Narayanan K, et al. Worldwide epidemiology of atrial fibrillation: a Global Burden of Disease 2010 study. Circulation 2014;129:837–47.

2. Miyasaka Y, Barnes ME, Gersh BJ, et al. Secular trends in incidence of atrial fibrillation in Olmsted County, Minnesota, 1980 to 2000, and implications on the projections for future prevalence. Circulation 2006;114:119–25.

3. Chamberlain AM, Agarwal SK, Ambrose M, et al. Metabolic syndrome and incidence of atrial fibrillation among blacks and whites in the Atherosclerosis Risk in Communities (ARIC) study. Am Heart J 2010;159:850–6.

4. Tedrow UB, Conen D, Ridker PM, et al. The long- and short-term impact of elevated body mass index on the risk of new atrial fibrillation the WHS (Women's Health Study). J Am Coll Cardiol 2010;55:2319–27.

5. Gami AS, Hodge DO, Herges RM, et al. Obstructive sleep apnea, obesity, and the risk of incident atrial fibrillation. J Am Coll Cardiol 2007;49:565–71.

6. Wang TJ, Parise H, Levy D, et al. Obesity and the risk of new-onset atrial fibrillation. JAMA 2004;292:2471–7.

7. Wanahita N, Messerli FH, Bangalore S, et al. Atrial fibrillation and obesity—results of a meta-analysis. Am Heart J 2008;155:310–5.

8. Abed HS, Samuel CS, Lau DH, et al. Obesity results in progressive atrial structural and electrical remodeling: implications for atrial fibrillation. Heart Rhythm 2013;10:90–100.

9. McCann JP, Bergman EN, Beermann DH. Dynamic and static phases of severe dietary obesity in sheep: food intakes, endocrinology and carcass and organ chemical composition. J Nutr 1992;122:496–505.

10. John B, Stiles MK, Kuklik P, et al. Electrical remodelling of the left and right atria due to rheumatic mitral stenosis. Eur Heart J 2008;29:2234–43.

11. Sanders P, Morton JB, Davidson NC, et al. Electrical remodeling of the atria in congestive heart failure: electrophysiological and electroanatomic mapping in humans. Circulation 2003;108:1461–8.

12. Li D, Fareh S, Leung TK, et al. Promotion of atrial fibrillation by heart failure in dogs: atrial remodeling of a different sort. Circulation 1999;100:87–95.

13. Lau DH, Mackenzie L, Kelly DJ, et al. Short-term hypertension is associated with the development of atrial fibrillation substrate: a study in an ovine hypertensive model. Heart Rhythm 2010;7:396–404.

14. Lau DH, Mackenzie L, Kelly DJ, et al. Hypertension and atrial fibrillation: evidence of progressive atrial remodeling with electrostructural correlate in a conscious chronically instrumented ovine model. Heart Rhythm 2010;7:1282–90.

15. Alasady M, Shipp NJ, Brooks AG, et al. Myocardial infarction and atrial fibrillation: importance of atrial ischemia. Circ Arrhythm Electrophysiol 2013;6:738–45.

16. Sanders P, Morton JB, Kistler PM, et al. Electrophysiological and electroanatomic characterization of the atria in sinus node disease: evidence of diffuse atrial remodeling. Circulation 2004;109:1514–22.

17. Dimitri H, Ng M, Brooks AG, et al. Atrial remodeling in obstructive sleep apnea: implications for atrial fibrillation. Heart Rhythm 2012;9:321–7.

18. Iwasaki YK, Shi Y, Benito B, et al. Determinants of atrial fibrillation in an animal model of obesity and acute obstructive sleep apnea. Heart Rhythm 2012;9:1409–16.e1.

19. Munger TM, Dong YX, Masaki M, et al. Electrophysiological and hemodynamic characteristics associated with obesity in patients with atrial fibrillation. J Am Coll Cardiol 2012;60:851–60.

20. Lau DH, Psaltis PJ, Mackenzie L, et al. Atrial remodeling in an ovine model of anthracycline-induced nonischemic cardiomyopathy: remodeling of the same sort. J Cardiovasc Electrophysiol 2011;22:175–82.

21. Spach MS, Boineau JP. Microfibrosis produces electrical load variations due to loss of side-to-side cell connections: a major mechanism of structural heart disease arrhythmias. Pacing Clin Electrophysiol 1997;20:397–413.

22. Verheule S, Sato T, Everett T 4th, et al. Increased vulnerability to atrial fibrillation in transgenic mice with selective atrial fibrosis caused by overexpression of TGF-beta1. Circ Res 2004;94:1458–65.

23. Fain JN, Tichansky DS, Madan AK. Transforming growth factor beta1 release by human adipose tissue is enhanced in obesity. Metabolism 2005;54:1546–51.

24. Weil BR, Westby CM, Van Guilder GP, et al. Enhanced endothelin-1 system activity with overweight and obesity. Am J Physiol Heart Circ Physiol 2011;301:H689–95.

25. Thanassoulis G, Massaro JM, O'Donnell CJ, et al. Pericardial fat is associated with prevalent atrial fibrillation: the Framingham Heart Study. Circ Arrhythm Electrophysiol 2010;3:345–50.

26. Batal O, Schoenhagen P, Shao M, et al. Left atrial epicardial adiposity and atrial fibrillation. Circ Arrhythm Electrophysiol 2010;3:230–6.

27. Al Chekakie MO, Welles CC, Metoyer R, et al. Pericardial fat is independently associated with human atrial fibrillation. J Am Coll Cardiol 2010;56:784–8.

28. Wong CX, Abed HS, Molaee P, et al. Pericardial fat is associated with atrial fibrillation severity and ablation outcome. J Am Coll Cardiol 2011;57:1745–51.

29. Sun K, Halberg N, Khan M, et al. Selective inhibition of hypoxia-inducible factor 1α ameliorates adipose tissue dysfunction. Mol Cell Biol 2013;33:904–17.

30. Venteclef N, Guglielmi V, Balse E, et al. Human epicardial adipose tissue induces fibrosis of the atrial myocardium through the secretion of adipofibrokines. Eur Heart J 2015;36:795–805.

KEY WORDS atrial fibrillation, epicardial fat, fibrosis, obesity, TGF-β1

APPENDIX For a supplemental Methods section, please see the online version of this article.